



MATRIX PATHOBIOLOGY

Type VIII Collagen Mediates Vessel Wall Remodeling after Arterial Injury and Fibrous Cap Formation in Atherosclerosis

Joshua Lopes,* Eser Adiguzel,* Steven Gu,[†] Shu-Lin Liu,[‡] Guangpei Hou,* Scott Heximer,[†] Richard K. Assoian,[‡] and Michelle P. Bendeck*[†]

From the Departments of Laboratory Medicine and Pathobiology* and Physiology,[†] University of Toronto, Toronto, Ontario, Canada; and the Department of Pharmacology,[‡] University of Pennsylvania, Philadelphia

Accepted for publication
February 12, 2013.

Address correspondence to
Michelle Bendeck, Ph.D.,
Department of Laboratory
Medicine and Pathobiology,
University of Toronto, 1 King's
College Circle, Rm. 6213, Tor-
onto, ON, Canada M5S 1A8.
E-mail: michelle.bendeck@
utoronto.ca.

Collagens in the atherosclerotic plaque signal regulation of cell behavior and provide tensile strength to the fibrous cap. Type VIII collagen, a short-chain collagen, is up-regulated in atherosclerosis; however, little is known about its functions *in vivo*. We studied the response to arterial injury and the development of atherosclerosis in type VIII collagen knockout mice (*Col8^{-/-}* mice). After wire injury of the femoral artery, *Col8^{-/-}* mice had decreased vessel wall thickening and outward remodeling when compared with *Col8^{+/+}* mice. We discovered that apolipoprotein E (ApoE) is an endogenous repressor of the Col8a1 chain, and, therefore, in ApoE knockout mice, type VIII collagen was up-regulated. Deficiency of type VIII collagen in *ApoE^{-/-}* mice (*Col8^{-/-};ApoE^{-/-}*) resulted in development of plaques with thin fibrous caps because of decreased smooth muscle cell migration and proliferation and reduced accumulation of fibrillar type I collagen. In contrast, macrophage accumulation was not affected, and the plaques had large lipid-rich necrotic cores. We conclude that in atherosclerosis, type VIII collagen is up-regulated in the absence of ApoE and functions to increase smooth muscle cell proliferation and migration. This is an important mechanism for formation of a thick fibrous cap to protect the atherosclerotic plaque from rupture. (*Am J Pathol* 2013, 182: 2241–2253; <http://dx.doi.org/10.1016/j.ajpath.2013.02.011>)

Collagens are the most abundant constituents of the extracellular matrix in atherosclerotic and restenotic vascular lesions and can be detrimental by contributing to lesion bulk and by signaling regulation of the migration and proliferation of vascular cells. However, collagens can also provide tensile strength to the fibrous cap and protect against plaque rupture, a devastating complication of atherosclerosis.¹

Type VIII collagen, a member of the short-chain non-fibrillar collagen family, is comprised of $\alpha 1$ and $\alpha 2$ collagen chains. It is present in small amounts in normal arteries; however, synthesis is dramatically increased after injury and during development of atherosclerosis in experimental animals and humans.^{2–10} *In vitro* studies have revealed that type VIII collagen is produced by both macrophages and smooth muscle cells (SMCs) and is stimulated by some atherogenic growth factors and cytokines.^{3,11–13} Type VIII collagen can act as a haptotactic factor for SMCs.¹⁴ Moreover, SMCs derived from type VIII collagen knockout mice migrate and proliferate less and express less matrix

metalloproteinase (MMP) activity than do cells from wild-type mice.¹⁵ Type VIII collagen-null SMCs were unable to overcome strong adhesion to interstitial type I collagen; however, adding exogenous type VIII collagen to the cultures rescued migration and proliferation. We concluded that type VIII collagen functioned as a provisional matrix masking the interstitial matrix and enabling SMCs to move in response to injury. Despite these *in vitro* data, there are few functional studies of type VIII collagen *in vivo*. After discontinuing a high-fat diet in a rabbit model of atherosclerosis, Plenz et al⁹ demonstrated a correlation between plaque regression, decreased type VIII collagen expression, and decreased macrophage accumulation in the adventitia.

Supported by grants MOP12604 and MOP81305 from the Canadian Institutes of Health Research (M.P.B.) and NIH grant HL62250 (R.K.A.). M.P.B. is a Career Investigator of the Heart and Stroke Foundation of Ontario. J.L. and E.A. are recipients of Ontario Graduate Scholarships.

Current address of E.A.: LasikMD, 1250 René-Lévesque Blvd. W, MD Level, Montréal, QC, Canada H3B 4W8.

However, those investigators did not determine cause-effect relationships between cholesterol, type VIII collagen, and macrophage accumulation, and they did not explore the underlying mechanisms. In current studies, we use knockout mice to investigate the functions of type VIII collagen *in vivo* using models of mechanical vascular injury and the apolipoprotein E (ApoE)—null mouse model of atherosclerosis.

ApoE is associated with very low-, intermediate-, and high-density lipoproteins and facilitates their clearance from plasma, and also mediates cholesterol efflux from vessel wall macrophages.¹⁶ Loss-of-function mutations in *apoE* have been linked to atherosclerosis in humans, and extensive experimental studies in ApoE-null mice have revealed important functions for this apolipoprotein in atherosclerosis, vascular remodeling, and restenosis. There is also evidence for cholesterol-independent effects of ApoE on SMCs, which could protect against atherosclerosis. For example ApoE can inhibit SMC proliferation through up-regulation of nitric oxide¹⁷ and the production of prostacyclin¹⁸; however, few studies have documented protective effects *in vivo*.

In present studies, we show that vessel wall thickening and outward remodeling of vessel diameter are attenuated after wire injury of the femoral artery in type VIII collagen knockout mice. We report here for the first time a direct effect of ApoE in suppression of type VIII collagen gene expression by SMCs; consequently, type VIII collagen gene expression is substantially increased in the *ApoE*^{-/-} mouse. Deficiency of type VIII collagen in the *ApoE*^{-/-} mouse results in impaired SMC proliferation and migration and decreased type I collagen accumulation, resulting in thinning of the fibrous cap. These studies point to an important role for type VIII collagen in mediating fibrous cap formation, which stabilizes atheromas.

Materials and Methods

Femoral Artery Injury in *Col8*^{+/+} and *Col8*^{-/-} Mice

Mice with targeted deletion of both the *col8a1* and *col8a2* genes (*Col8*^{-/-} mice) backcrossed more than 10 generations in the C57BL/6 strain were generated in the laboratory of Dr. Bjorn Olsen (Harvard Medical School), as previously described,¹⁹ and were generously provided for these experiments. Animal experiments were approved by the local animal care committee at the University of Toronto in accordance with the *Guide for the Care and Use of Laboratory Animals* (NIH Publ No. 85-23, revised 1996). The University of Toronto is compliant with the NIH guide (A5013-01). Before surgery, male mice were injected subcutaneously with 0.1 mg/kg buprenorphine, then anesthetized via inhalation of 1.5% to 2% isoflurane in oxygen, 1.5 L/min. Anesthesia was monitored by observation of breathing rate and pinching between the toes on the paw. Wire injury of the femoral artery was performed by

introducing a 0.38-mm diameter straight spring wire into a small branch artery of the femoral artery and advancing it through the femoral artery >5 mm toward the iliac artery. The wire was left in place for 1 minute to denude the endothelium and dilate the artery.²⁰ Mice were sacrificed at either 7 or 21 days after injury via intraperitoneal injection of ketamine, 333 mg/kg body weight (Ayerst Veterinary Laboratories; Guelph, ON, Canada), and xylazine, 67 mg/kg body weight (Bayer, Inc., Toronto, ON, Canada). The entire circulatory system was perfused at constant physiologic pressure via a catheter placed in the left ventricle, first with 0.9% saline solution (Baxter Corp., Mississauga, ON, Canada) and then with 4% paraformaldehyde for 10 minutes. The femoral artery, extending from the iliac artery to the ligated small branch artery, was removed, placed in 4% paraformaldehyde for 2 hours, then transferred to PBS. The vessels were bisected, then paraffin embedded. Cross-sections (4 μm) were cut from each bisected half to obtain an accurate representation of injury along the length of the femoral artery, and analysis was performed on cross-sections from the middle of the femoral arteries. Tissue processing was performed by the Centre for Modeling Human Disease Pathology Core, the Toronto Centre for Phenogenomics (Toronto, ON, Canada). With use of digital imaging (Simple PCI software version 5.3; Compix, Inc., Mars PA), cross-sectional areas of the neointima and media and vessel wall cell numbers and vessel diameters were measured in sections obtained at 21 days after injury. Sections from uninjured control femoral arteries served as controls. Cell proliferation was detected by immunostaining for Ki-67, and apoptosis by TUNEL in sections obtained at 7 days after injury. Values from *Col8*^{-/-} mice were compared with those from *Col8*^{+/+} control mice.

Ki-67 is a nuclear antigen associated with proliferation and is present during the cell cycle but absent during the resting G₀ phase. Sections were stained with a 1:200 dilution of rabbit anti-Ki-67 antibody (No. RM-9106-S; Lab Vision Corp., Fremont, CA), then with biotin-conjugated goat anti-rabbit IgG secondary antibody (No. BA-1000; Vector Laboratories, Inc., Burlingame, CA), and were visualized with 3,3'-diaminobenzidine and counterstained with hematoxylin. The percentage of Ki-67-labeled nuclei was measured in the medial layer of the vessel using an Eclipse E600 microscope (Nikon Corp., Tokyo, Japan), a camera (Hamamatsu Photonics KK, Hamamatsu City, Japan), and Simple PCI software (Compix).

A TUNEL assay was performed to measure the percentage of apoptotic cells, using a kit from Millipore (Canada), Ltd. (Etobicoke, ON, Canada). Tissues were deparaffinized in a series of xylene washes and rehydrated in ethanol. The tissue was digested with 0.02 mg/mL proteinase K to inactivate nucleases. The slides were then pretreated with an equilibration buffer for 15 minutes, followed by incubation for 1 hour at 37°C in the terminal deoxynucleotidyl transferase enzyme reaction mixture. Sections were treated with stop/wash buffer for 25 minutes, incubated with a fluorescein-tagged anti-

digoxigenin antibody for 30 minutes, and counterstained with 0.5 µg/mL propidium iodide. The percentage of TUNEL-positive cells in the medium was determined using an Eclipse E600 microscope, DS-Fi1 camera, and NIS-Elements software (all from Nikon).

mRNA Isolation from Male C57BL/6 or *ApoE*^{-/-} Mouse Aortas

Aortas were isolated from 24-week-old male C57BL/6 or *ApoE*^{-/-} mice. Aortas were dissected, and extraneous tissue from the adventitial side was carefully removed. Aortas were divided into arch (ascending) and thoracic (descending) regions and stabilized by submerging the tissues in RNAlater (Qiagen GmbH, Hilden, Germany). Before isolating the total RNA, the aortas were weighed, and approximately 10 mg aortic tissue was manually homogenized and treated with 10 mg/mL proteinase K (Qiagen) at 55°C for 10 minutes. The homogenate was clarified via centrifugation, and total RNA was isolated from the supernatant using RNeasy mini columns (Qiagen).

Cell Culture and Lipoprotein Treatment

Primary murine aortic SMCs were isolated from C57BL/6 mice and used between passages 2 and 5. The SMCs were grown to 80% to 90% confluence and were serum-starved via incubation in Dulbecco's Minimum essential's medium containing 1 mg/mL heat-inactivated fatty acid-free bovine serum albumin for 48 hours. The quiescent cells were stimulated with 10% fetal bovine serum in the absence or presence of 2 µmol/L recombinant apolipoprotein or 50 µg/mL lipoprotein (generous gift of Drs. Michael C. Phillips and Sissel Lund-Katz, Children's Hospital of Philadelphia) for 24 hours. Total RNA was isolated from cells lysed in Trizol reagent (Invitrogen Corp., Carlsbad, CA) and analyzed using real-time quantitative RT-PCR (RT-qPCR), as outlined in the following section.

Real-Time RT-qPCR

Real-time RT-qPCR was performed as described,²¹ using 50 to 100 ng for reverse transcription of total RNA isolated from cultured SMCs or aortas. A 10% aliquot of cDNA was prepared using SYBR Green QPCR Master Mix (Applied Biosystems, Inc., Foster City, CA) to qPCR with 900 nmol/L of the primer-probe sets mCOL8A1 (forward, 5'-AGAGTGCACCCAGCCCCAGT-3'; reverse, 5'-TGG-GTGGCACAGCCATCACATTT-3') and mCOL8A2 (forward, 5'-CCTGCAGGCTCTGCCTGTCC-3'; reverse, 5'-CACTCTTGCCCCACACCCCA-3'). RT-qPCR results were calculated using 18S rRNA as the reference for mRNAs. To detect mouse 18S rRNA, we used TaqMan Universal PCR Master Mix (Applied Biosystems) with forward primer 5'-CCTGGTTGATCCTGCCAGTAG-3', reverse primer 5'-CCGTGCGTACTTAGACATGCA-3', and probe 5'-VIC-

TGCTGTCTCAAAGATTA-MGB-NFQ-3'. Each sample was analyzed in duplicate PCR reactions, and mRNA expression was quantified against a standard curve using ABI PRISM 7000 SDS software (Applied Biosystems). Mean quantities and SD were calculated from duplicate PCR reactions.

Generation of *Col8*^{-/-};*ApoE*^{-/-} Mice

Col8^{-/-} mice were bred with *ApoE*^{-/-} mice (both on C57BL/6 background) to generate mice that were *Col8*^{-/-};*ApoE*^{-/-}. These were compared with either littermate control *Col8*^{+/+};*ApoE*^{-/-} mice or *ApoE*^{-/-} mice (purchased from The Jackson Laboratory, Bar Harbor, ME). Genomic DNA was extracted from ear clips, and genotyping was performed via PCR amplification using the following primers: *Col8a1* wild type: sense, 5'-CGGGAGTAGGAAAACCAGGAGTGA-3', and antisense, 5'-GGCCCAAGAACCCAGGAACA-3'; *Col8a1* knockout: sense, 5'-GTGGGGTGGGGTGGGAT-TAGATA-3', and antisense, 5'-CTCGGCCAAGAACCC-AGGAAC-3'; *Col8a2* wild type: sense, 5'-CCGGTAAAG-TATGTGCAGC-3', and antisense, 5'-CAAGTCCATTGG-CAGCATC-3'; *Col8a2* knockout: sense, 5'-CAGCGCATC-GCCTTCTATCGC-3', and antisense identical to wild-type *Col8a2*; *ApoE* wild type: sense, 5'-GCCTAGCCGAGGGA-GAGCCG-3', and antisense, 5'-TGTGACTTGGGAGCTC-TGCAGC-3'; *ApoE* knockout: sense, same as wild type, and antisense, 5'-GCCGCCCCGACTGCATCT-3'. Beginning at age 8 to 12 weeks, male and female mice of both genotypes were fed an atherogenic diet containing 40% kcal fat and 1.25% cholesterol by weight (D12108; Research Diets, Inc., New Brunswick, NJ) for 6 or 12 weeks. On the day when sacrificed, mice were euthanized via CO₂ asphyxiation. The left ventricle was cannulated, and animals were perfused at physiologic pressure (100 mmHg), first with sterile saline solution and then with 4% paraformaldehyde for 5 to 10 minutes. The aortic arch and descending aorta to the iliac bifurcation were isolated, cleared of fat and surrounding tissues, and used as described below to measure oil-red-o staining, immunohistochemistry, matrix staining and plaque architecture, and in situ zymography. For analyses that required fresh-frozen tissues, mice were perfused with sterile saline solution, and arterial tissues were immediately dissected in PBS, embedded in OCT, and snap frozen in liquid nitrogen.

Mean Arterial Pressure

Mean arterial pressure was measured after 6 and 12 weeks of the atherogenic diet via catheterization of the right common carotid artery using a 1.4F blood pressure probe (Millar Instruments, Inc., Houston, TX). Mice were anesthetized using 3% isoflurane, the carotid artery was catheterized, and blood pressure was allowed to stabilize for 3 minutes with 1% isoflurane. Measurement of blood pressure was performed for 1 minute, and mean arterial pressure was calculated using the following formula: Mean arterial pressure = Diastolic blood pressure + 1/3 Pulse pressure.

Plasma Lipid Analysis

Whole blood samples were collected at sacrifice via right ventricle puncture and placed in heparinized 1.5-mL tubes. Blood samples were spun at $14,800 \times g$ for 5 minutes at 4°C and were stored at 4°C for a maximum of 2 days before analysis. Plasma samples were analyzed using a multiplate spectrophotometer (Microscan; Titertek Instruments, Inc., Huntsville, AL) at 492 nm using enzymatic assays (Synchro; Beckman Coulter, Inc., Brea, CA) for triglycerides (kit No. 445850) and total cholesterol (kit No. 467825).

Oil Red O Staining

Atherosclerotic plaque burden in the descending aorta (downstream of the left subclavian artery to the iliac bifurcation) was determined via Oil Red O staining. Aortas were incised longitudinally, pinned *en face* to black silicone plates using 0.1-mm minuten pins, rinsed with isopropanol, and stained with 18 mg/mL Oil Red O for 30 minutes at room temperature on a shaker. Stained aortas were washed three or four times in 70% isopropanol and imaged using a CoolPix digital camera (Nikon). The percentage of Oil Red O-positive plaque per total aortic surface area was quantified using digital image analysis (NIS-Elements Basic Research; Nikon).

Immunohistochemistry, Matrix Staining, and Plaque Architecture

Paraformaldehyde-fixed, paraffin-embedded longitudinal sections of the mouse aortic arch including the brachiocephalic and left carotid artery branchpoints were deparaffinized in xylenes, rehydrated in an ethanol series, and blocked using 0.3% H_2O_2 in cold methanol, followed by a 1% bovine serum albumin blocking solution (kit No. D12287; Invitrogen). Primary antibodies directed against mouse α -smooth muscle actin raised in goat (1:500) (A2547; Sigma; St. Louis, MO), mouse Mac-2 raised in rat (1:100) (CL8942AP; Cedarlane Laboratories USA, Inc., Burlington, NC), or type I collagen raised in rabbit (1:200) (ab21286; Abcam plc, Cambridge, MA) were used to stain for SMCs, macrophages, and type I collagen, respectively. Negative controls included sections incubated without primary antibody. Slides were then incubated with species-specific biotinylated secondary antibodies including anti-goat (1:4000) (B2763; Invitrogen), anti-rat (1:200) (E0468; DakoCytomation Inc., Carpinteria, CA), and anti-rabbit (1:1000) (B2770; Invitrogen), followed by incubation in streptavidin-horseradish peroxidase-conjugated solution following the manufacturer's instructions (kit No. D12287; Invitrogen). Sections were then incubated in 3,3'-diaminobenzidine (kit No. D12287; Invitrogen), a chromogenic substrate, followed by counterstaining with hematoxylin. Serial sections were stained using Picosirius Red (PSR) for collagen and either Verhoeff-Van Geisin stain or Movat's pentachrome stain for elastin. Whole

plaques located on the lesser curvature of the arch and in the brachiocephalic and left carotid artery branchpoints were measured. Plaque area was defined as the region extending from the internal elastic lamina to the luminal edge of the plaque. Thresholding of maximum and minimum color intensity was conducted using NIS-Elements Basic Research software (Nikon), with positively stained regions expressed as a percentage of plaque area. Fibrous cap thickness and necrotic core area were assessed using PSR-stained longitudinal sections of lesser curvature plaques. Relative fibrous cap thickness was calculated by dividing fibrous cap thickness by the entire height of the plaque (from the internal elastic lamina to the luminal edge). Necrotic core area was measured as a percentage of total plaque area. The percentage of area stained positive for SMCs and collagen was also assessed independently in the plaque fibrous cap. Ki-67 and TUNEL assays were performed as described (see *Femoral Artery Injury in Col8^{+/+} and Col8^{-/-} Mice*). PSR- and Movat's pentachrome-stained plaque sections from the lesser curvature were ranked according to criteria established by Virmani et al.²² The percentage of samples with plaques in each of the five categories (no plaques, intimal xanthoma, pathologic intimal thickening, fibrous cap atheroma, and thin fibrous cap atheroma) was plotted for *Col8^{+/+};Apoe^{-/-}* and *Col8^{-/-};Apoe^{-/-}* mice.

Fluorescence *in Situ* Zymography

In situ examination of gelatinase activity was performed using fluorescence-quenched gelatin (DQ-Gelatin, No. D12054; Invitrogen). Gelatinase-catalyzed hydrolysis of the molecule relieves the quenching, and the magnitude of the resultant fluorescence is proportional to the extent of proteolytic digestion. Longitudinal cryosections (8 μm long) of mouse aortic arch were washed in ISZ incubation buffer [50 mmol/L Tris-HCl (pH 7.8), 150 mmol/L NaCl, 5 mmol/L CaCl_2 , and 0.2 mmol/L NaN_3] and incubated overnight at 4°C in incubation buffer. The sections were then counterstained for 10 minutes with Hoechst 33258 diluted 1:10,000 in incubation buffer. A prewarmed solution of incubation buffer containing 0.1% agarose and 0.1 mg/mL fluorescence-quenched gelatin was applied to the sections, which were then coverslipped and incubated for 30 minutes at 37°C . Images of the lesser curvature plaque were acquired using an E600 Epifluorescence Microscope using a filter set with excitation of 465 to 495 nm and emission of 515 to 555 nm, and a DS-Fi1 camera with NIS-Elements software (all from Nikon), with exposure time set to 2 seconds and gain set to 9.60. All sections were imaged under the same conditions. Samples were ranked for gelatinase activity on a scale of 1 to 4.

Statistical Analysis

All animal experiments were performed with the experimenter blinded to the genotype of the mice (J.L., E.A., G.H.

and M.P.B.). Data were analyzed using Student's *t*-test (comparing two groups) or analysis of variance (comparing multiple groups). After analysis of variance, Student-Newman-Keuls post hoc tests were used to determine statistically significant differences between groups, with a significance level of $P \leq 0.05$. For data that did not fit a normal distribution and ranked data, the nonparametric *U*-test was used to compare the means between two groups.

Results

Vessel Wall Thickening and Outward Remodeling Is Reduced in *Col8*^{-/-} Mice after Femoral Artery Injury

In previous studies, we and others have shown that type VIII collagen expression was up-regulated after endothelial denuding injury^{2,3,6}; however, these studies merely described a correlation and did not address the functions of type VIII collagen in the injured vessel. To investigate, we used a wire to denude the endothelium in the femoral arteries of *Col8*^{+/+} and *Col8*^{-/-} mice. In the absence of injury, there were no significant differences in medial SMC number, medial area, or vessel diameter between *Col8*^{+/+} and *Col8*^{-/-} mice (Table 1). The response to arterial injury involves thickening of both intimal and medial layers and outward remodeling of vessel diameter.^{20,23} The response to injury in the *Col8*^{+/+} mice included thickening of the medial and intimal layers and outward remodeling of arterial diameter. In contrast, these responses were significantly attenuated after injury of the femoral arteries from *Col8*^{-/-} mice. Cross-sections of femoral arteries obtained at 21 days after injury (Figure 1, A and B) showed a pronounced reduction in vessel thickening and smaller vessel diameter in *Col8*^{-/-} mice compared with *Col8*^{+/+} mice. Cell numbers in the medial and intimal layers were reduced in *Col8*^{-/-} mice compared with *Col8*^{+/+} mice (Figure 1C), as were cross-sectional area of the vessel wall (Figure 1D) and vessel diameter (Figure 1E). The decreased vessel diameter is indicative of attenuated outward remodeling of the vessel in *Col8*^{-/-} mice.

The reductions in cell numbers in media and intima and the reduction in total vessel wall area in *Col8*^{-/-} mice could be the result of either decreased cell migration or proliferation or of increased apoptosis. We assessed SMC proliferation by immunostaining for Ki-67 (Figure 1, H and I) and found that proliferation was increased in *Col8*^{-/-} mice compared with *Col8*^{+/+} mice (Figure 1F). TUNEL labeling

revealed a trend toward increased apoptosis in the *Col8*^{-/-} mice (Figure 1G). Ki-67- and TUNEL-labeled cells were distributed throughout the media of the injured arteries. Considered together, the data suggest that reduced vessel wall thickening in the *Col8*^{-/-} mice was not due to a reduction in SMC proliferation but to a combination of increased SMC apoptosis and decreased SMC migration to the intimal layer.

Type VIII Collagen Is Up-regulated in *ApoE*^{-/-} Mice

The femoral injury model lacks many of the complications of atherosclerosis as there is little inflammation and no lipid infiltration in the vessel wall. To investigate type VIII collagen in a more complex model of vascular disease, we used the *ApoE*^{-/-} mouse model of atherosclerosis. First we used RT-qPCR to measure mRNA for the $\alpha 1$ and $\alpha 2$ chains of type VIII collagen in isolated aortic arches and thoracic aortas from C57Bl/6 wild-type and *ApoE*^{-/-} mice. This revealed a fivefold increase in *Col8a1* mRNA in *ApoE*^{-/-} mice at age 24 weeks (Figure 2A). In contrast, levels of mRNA for the *Col8a2* chain were much lower and did not differ between wild-type and *ApoE*^{-/-} mice (Figure 2A). Moreover, we found that *Col8a1* mRNA was elevated as early as age 8 weeks in the *ApoE*^{-/-} mice (Supplemental Figure S1A). To determine whether the changes in type VIII collagen gene expression were the result of a direct effect of ApoE, primary mouse SMCs in culture were treated with ApoE3, high-density lipoprotein (HDL), ApoA1, or low-density lipoprotein (LDL). ApoE3 or HDL suppressed *Col8a1* mRNA, whereas ApoA1 or LDL (used as controls) had no effect (Figure 2B). In contrast, treatment with ApoE3 did not affect expression of mRNA for the *Col8a2* chain, which was expressed at much lower levels than *Col8a1* (Supplemental Figure S1B).

Plaque Size and Burden of Atherosclerosis Is Similar in *Col8*^{-/-}; *ApoE*^{-/-} and *Col8*^{+/+}; *ApoE*^{-/-} Mice

To study the role of type VIII collagen in atherosclerotic plaque progression, we crossed *Col8*^{+/+} and *Col8*^{-/-} mice with *ApoE*^{-/-} mice to generate mice that were either *Col8*^{+/+}; *ApoE*^{-/-} or *Col8*^{-/-}; *ApoE*^{-/-}. To accelerate progression of atherosclerosis, all mice were fed an atherogenic diet, starting at age 8 to 12 weeks and continuing for another 6 or 12 weeks. Body weight, heart rate, mean arterial pressure, and plasma triglyceride concentrations were not significantly different between the genotypes (Table 2). There was a transient increase in plasma cholesterol concentration in the *Col8*^{-/-}; *ApoE*^{-/-} mice compared with the *Col8*^{+/+}; *ApoE*^{-/-} mice at 6 weeks of the atherogenic diet; however, this difference was resolved by 12 weeks (Table 2).

Atherosclerotic plaque area was measured on longitudinal sections taken from the lesser curvature of the aortic arch and at the branchpoints of the brachiocephalic and left

Table 1 Data for Uninjured Femoral Arteries

Variable	<i>Col8</i> ^{+/+} mice (n = 4)	<i>Col8</i> ^{-/-} mice (n = 4)
Medial cell number	58.7 ± 10.3	54.2 ± 4.3
Medial area (μm ²)	11849 ± 1087	10202 ± 665
Diameter (μm)	315.8 ± 9.5	312.8 ± 9.3

Values represent means ± SEM.

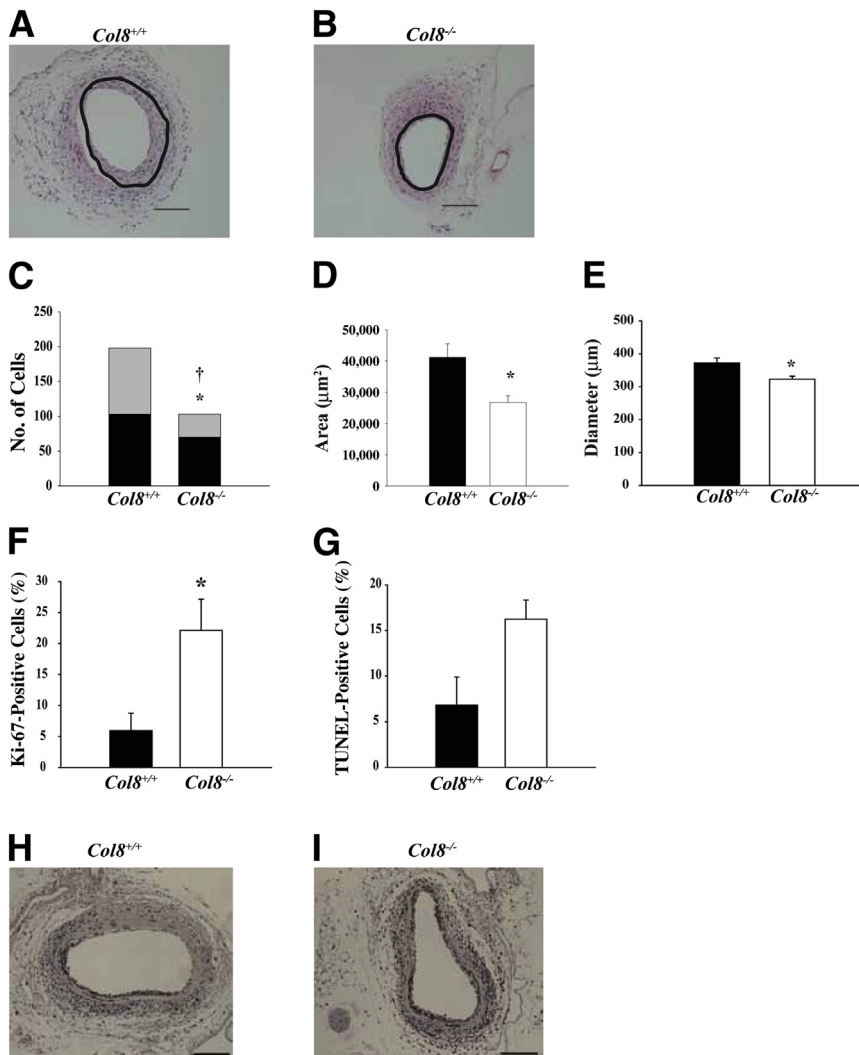


Figure 1 Vessel wall thickening, cell number, and vessel diameter are reduced, but apoptosis and proliferation are increased after injury of the femoral artery in *Col8^{-/-}* mice. **A** and **B**: Representative cross-sections of injured femoral arteries from *Col8^{+/+}* and *Col8^{-/-}* mice, respectively, at 21 days after injury. **Black circles** show the location of the internal elastic lamina. Scale bars: 200 μm. **C**: Cell number in the media (black bars) and intima (gray bars) and total cell number (sum of black and gray bars) in *Col8^{+/+}* ($n = 14$) and *Col8^{-/-}* ($n = 12$) mice at 21 days after injury. * $P \leq 0.05$, significant difference in medial cell number between genotypes. † $P \leq 0.05$, difference in total cell number between genotypes. **D**: Vessel wall medial and neointimal area at 21 days after wire injury. **E**: Vessel diameter at 21 days after wire injury. **F**: Cell proliferation in the media measured at 7 days after injury via Ki-67 immunostaining of sections from *Col8^{+/+}* ($n = 3$) and *Col8^{-/-}* ($n = 4$) mice. **G**: Apoptosis was quantified by measuring the percentage of TUNEL-positive cells in the media at 7 days in *Col8^{+/+}* ($n = 3$) and *Col8^{-/-}* ($n = 3$) mice. **D–G**: Black bars represent the values from *Col8^{+/+}* mice, and white bars represent the values from *Col8^{-/-}* mice. * $P \leq 0.05$. **H** and **I**: Representative cross-sections of injured femoral arteries from *Col8^{+/+}* mice (**H**) and *Col8^{-/-}* mice (**I**), respectively, at 7 days after injury, stained for Ki-67. Scale bars: 100 μm.

carotid arteries. Representative sections of aortic arch plaques at 6 and 12 weeks are shown in **Figure 3**, **A** and **B**. At neither time point were there significant differences in plaque area in the aortic arch (**Figure 3C**), brachiocephalic artery (**Figure 3D**), or left carotid artery (**Figure 3E**) between *Col8^{+/+};Apoe^{-/-}* and *Col8^{-/-};Apoe^{-/-}* mice. Total plaque burden was measured along the length of the descending aorta by staining with Oil Red O and imaging the aortas *en face*, then calculating the percentage of aortic surface area covered by plaque. Plaque burden did not differ significantly between the genotypes at either time point measured (**Figure 3F**).

SMC Accumulation Is Reduced in Plaques from *Col8^{-/-};Apoe^{-/-}* Mice

SMCs and macrophages are the main cell types present in the plaques of *Apoe^{-/-}* mice, and previous *in vitro* studies have demonstrated that both cell types are able to produce and respond to type VIII collagen.¹¹ To determine whether SMC or macrophage accumulation within the plaques was

affected by deletion of type VIII collagen, sections were immunostained using antibodies against SMA and Mac-2. Representative 12-week plaque sections are shown in **Figure 4**, **A** and **B**. Accumulation of SMCs was reduced in *Col8^{-/-};Apoe^{-/-}* mice compared with *Col8^{+/+};Apoe^{-/-}* mice after ingestion of an atherogenic diet for 6 or 12 weeks (**Figure 4C**). In contrast, accumulation of macrophages did not differ between genotypes at either time point (**Figure 4D**). Most of the foam cells in the plaque stained positive for Mac-2, which suggests that these cells were derived from plaque macrophages. We performed Ki-67 and TUNEL labeling to measure cell proliferation and apoptosis, respectively. At 6 weeks, there was a decrease in cell proliferation in plaques from the *Col8^{-/-};Apoe^{-/-}* mice; however, by 12 weeks, there was no difference between genotypes (**Figure 4E**). In contrast, there were no genotype-dependent differences in apoptosis at either time point (**Figure 4F**). This suggests that decreased SMC accumulation in the plaques of *Col8^{-/-};Apoe^{-/-}* mice was due to decreased proliferation and migration, not to increased apoptosis.

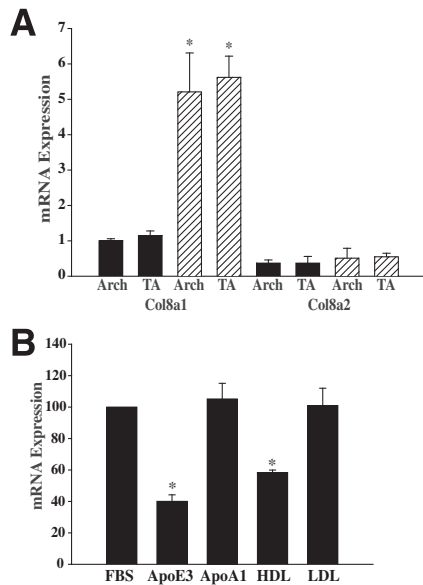


Figure 2 Expression of Col8a1 mRNA is suppressed by ApoE and HDL. **A:** mRNA levels for the $\alpha 1$ chain of type VIII collagen (Col8a1) were significantly increased in the aortic arch (Arch) and thoracic aorta (TA) of *ApoE*^{-/-} mice (hatched bars) compared with wild-type C57BL/6 mice (black bars). mRNA levels for the $\alpha 2$ chain of type VIII collagen (Col8a2) were low and did not differ between genotypes. All values are expressed as a fold change compared with levels of mRNA for Col8a1 in wild-type aortic arch. * $P \leq 0.05$ compared with corresponding wild-type aorta; $n = 4$ samples of aortic segments pooled from 3 to 4 mice each. **B:** Primary mouse SMCs were incubated in 10% FBS in the absence or presence of ApoE3, ApoA1, HDL, or LDL. mRNA expression for Col8a1 was measured using RT-qPCR and is expressed as a percentage of FBS control. * $P \leq 0.05$ compared with FBS control; $n = 4$ experiments.

Collagen and Elastin Accumulation Are Reduced in *Col8*^{-/-};*ApoE*^{-/-} Mice

Extracellular matrix composition was assessed by staining sections of aortic arch with PSR, which binds to collagen, or Verhoeff–Van Gieson stain, which stains elastin fibers black. Representative 12-week plaque sections stained with PSR or Verhoeff–Van Gieson stain are shown in Figure 5, A and B, respectively. Total collagen content was reduced in plaques from *Col8*^{-/-};*ApoE*^{-/-} mice compared with *Col8*^{+/+};*ApoE*^{-/-} mice at both 6 and 12 weeks (Figure 5C). Analysis of fibrillar collagen content and organization in the lesions was performed by measuring collagen fiber birefringence using the PolScope (Abrio IM Imaging System; Cambridge Research and Instrumentation, Inc., Woburn, MA). There was a significant decrease in fibrillar collagen in plaques from *Col8*^{-/-};*ApoE*^{-/-} mice at both time points (Figure 5D). Images from the PolScope show this reduction in organized fibrillar collagen in the 12-week plaques from *Col8*^{-/-};*ApoE*^{-/-} mice (Supplemental Figure S2, A and B). Immunostaining revealed a reduction in type I collagen in plaques from *Col8*^{-/-};*ApoE*^{-/-} mice (Supplemental Figure S2, C–E). Elastin content was reduced in plaques from *Col8*^{-/-};*ApoE*^{-/-} mice compared with *Col8*^{+/+};*ApoE*^{-/-} mice at 6 weeks; however, by 12 weeks, there was no difference between the genotypes (Figure 5E).

Plaques from *Col8*^{-/-};*ApoE*^{-/-} Mice Exhibit Thin Fibrous Caps and Increased Necrotic Core Size

The decreases in matrix and SMC accumulation in the *Col8*^{-/-};*ApoE*^{-/-} mice gave the appearance of thinner fibrous caps, and indeed we showed that relative fibrous cap thickness was decreased in *Col8*^{-/-};*ApoE*^{-/-} mice compared with *Col8*^{+/+};*ApoE*^{-/-} mice at 12 weeks (Figure 5F). Conversely, the percentage of plaque occupied by necrotic core was increased in plaques from *Col8*^{-/-};*ApoE*^{-/-} mice (Figure 5G). SMC content in the fibrous cap was decreased from (means \pm SD) 27.2% \pm 3.1% in *Col8*^{+/+};*ApoE*^{-/-} mice to 14.2% \pm 3.4% in *Col8*^{-/-};*ApoE*^{-/-} mice ($P \leq 0.05$). Collagen content of the fibrous cap was decreased from 39.5% \pm 5.7% in *Col8*^{+/+};*ApoE*^{-/-} mice to 23.4% \pm 4.0% in *Col8*^{-/-};*ApoE*^{-/-} mice ($P \leq 0.05$). There were no significant changes in macrophage content in the fibrous cap (data not shown). Considered together, these data indicate that SMC infiltration to form the fibrous cap was decreased, as was the amount of matrix deposited in the cap.

We classified plaque pathologic findings according to a scale developed by Virmani et al.²² In the *Col8*^{-/-};*ApoE*^{-/-} mice, there were greater percentages of plaques with features of intimal xanthomas (38%), pathologic intimal thickening (12%), and thinned fibrous caps (19%) than in the *Col8*^{+/+};*ApoE*^{-/-} mice (20%, 7%, and 13%, respectively) (Figure 5H). Conversely, the percentage of plaques with thick fibrous caps was greater in the *Col8*^{+/+};*ApoE*^{-/-} mice (47%) than in the *Col8*^{-/-};*ApoE*^{-/-} mice (12%). These data suggest that plaques in *Col8*^{-/-};*ApoE*^{-/-} mice might be vulnerable to rupture.

Gelatinase Activity Is Decreased in Plaques from *Col8*^{-/-};*ApoE*^{-/-} Mice

In atherosclerotic plaque, both SMCs and macrophages produce proteinases that facilitate cell migration but may also thin the fibrous cap by degrading matrix.²⁴ In the *Col8*^{-/-};*ApoE*^{-/-} mice, SMC accumulation was attenuated in the absence of a change in macrophage content. Therefore, development of plaques with thin fibrous caps could be due to either reduced SMC migration and proliferation to populate the cap and synthesize matrix or to increased degradation of matrix in the cap by the relatively abundant macrophages. To differentiate these possibilities, we assessed plaque gelatinase activity using *in situ* zymography. Frozen sections were overlaid with fluorescence-quenched gelatin substrate, which exhibits bright green fluorescence when cleaved. Gelatinase activity was prominent in the fibrous cap of plaques from *Col8*^{+/+};*ApoE*^{-/-} mice (Figure 6A). In contrast, gelatinase activity in the fibrous cap was markedly reduced in plaques from *Col8*^{-/-};*ApoE*^{-/-} mice (Figure 6B). We quantified this by ranking plaques on a scale of 1 to 4 (with 4 indicative of the highest fluorescence) and found that activity was substantially reduced in plaques from *Col8*^{-/-};*ApoE*^{-/-} mice (Figure 6C). This shows that gelatinolytic proteinases are produced by

Table 2 Systemic Variables for Mice Fed an Atherogenic Diet

Variable	Duration of atherogenic diet			
	6 Weeks		12 Weeks	
	<i>Col8^{+/+};ApoE^{-/-}</i>	<i>Col8^{-/-};ApoE^{-/-}</i>	<i>Col8^{+/+};ApoE^{-/-}</i>	<i>Col8^{-/-};ApoE^{-/-}</i>
Mean arterial pressure (mmHg)	66.3 ± 3.6 (n = 8)	61.3 ± 2.1 (n = 8)	70.4 ± 2.8 (n = 8)	66.4 ± 2.1 (n = 8)
Heart rate (beats/minute)	491 ± 19 (n = 8)	455 ± 14 (n = 8)	523 ± 28 (n = 8)	487 ± 14 (n = 8)
Body weight (g)	25.4 ± 1.1 (n = 15)	27.0 ± 0.9 (n = 18)	30.0 ± 1.1 (n = 13)	31.8 ± 1.3 (n = 17)
Plasma triglyceride concentration (mmol/L)	1.45 ± 0.16 (n = 9)	1.65 ± 0.19 (n = 12)	1.64 ± 0.09 (n = 10)	1.78 ± 0.16 (n = 13)
Plasma cholesterol concentration (mmol/L)	16.8 ± 1.2 (n = 9)	22.1 ± 1.3* (n = 12)	16.3 ± 1.0 (n = 10)	19.0 ± 1.2 (n = 13)

Values represent means ± SEM. Sample size is indicated in parentheses.

* $P \leq 0.05$

SMCs in the presence of type VIII collagen and are important for their migration to the fibrous cap.

Discussion

In the present study, we discovered an important function of type VIII collagen in regulating development of the fibrous cap in atheromas. Moreover, we are the first to show that type VIII collagen influences SMC proliferation, migration to the intima, cell survival, and deposition of fibrillar type I

collagen after vascular injury *in vivo*. Inasmuch as plaque rupture and subsequent thrombosis are responsible for most fatal acute myocardial infarctions, our results provide insight into an important endogenous protective mechanism in atherosclerosis.

The response to endothelial denuding injury in the femoral artery is characterized by cell proliferation and migration from media to intima, resulting in vessel wall thickening and outward expansion to increase vessel diameter.²⁰ Previous studies of endothelial denudation have shown that type VIII collagen was up-regulated in SMCs within the first layer of the

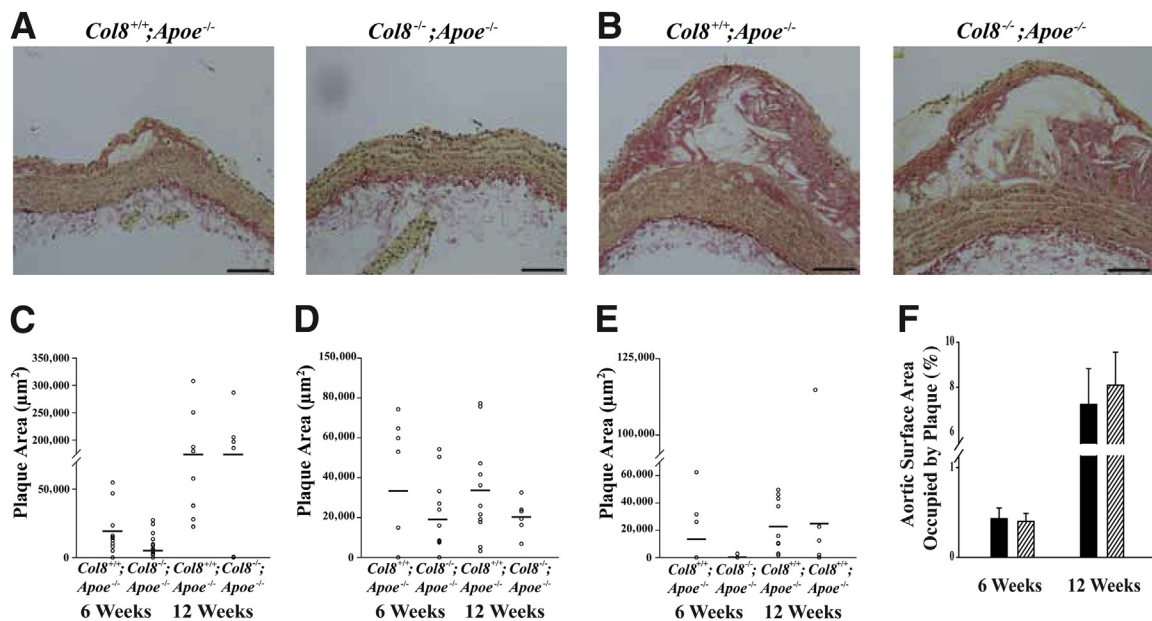


Figure 3 Atherosclerotic plaque size and total plaque burden does not differ between *Col8^{+/+};ApoE^{-/-}* and *Col8^{-/-};ApoE^{-/-}* mice. Representative longitudinal sections of aortic arches from *Col8^{+/+};ApoE^{-/-}* and *Col8^{-/-};ApoE^{-/-}* mice after 6 weeks (A) or 12 weeks (B) of an atherogenic diet. C: Plaque area was measured in the lesser curvature of the aortic arch after an atherogenic diet at 6 weeks in *Col8^{+/+};ApoE^{-/-}* (n = 13) and *Col8^{-/-};ApoE^{-/-}* (n = 17) mice or at 12 weeks in *Col8^{+/+};ApoE^{-/-}* (n = 13) and *Col8^{-/-};ApoE^{-/-}* (n = 15) mice. D: Plaque area was measured in the brachiocephalic artery at 6 weeks in *Col8^{+/+};ApoE^{-/-}* (n = 8) and *Col8^{-/-};ApoE^{-/-}* (n = 12) mice or at 12 weeks in *Col8^{+/+};ApoE^{-/-}* (n = 11) and *Col8^{-/-};ApoE^{-/-}* (n = 6) mice. E: Plaque area was measured in the left common carotid artery at 6 weeks in *Col8^{+/+};ApoE^{-/-}* (n = 9) and *Col8^{-/-};ApoE^{-/-}* (n = 9) mice or at 12 weeks in *Col8^{+/+};ApoE^{-/-}* (n = 10) and *Col8^{-/-};ApoE^{-/-}* (n = 6) mice. Horizontal lines indicate the group mean. F: The percentage of descending aorta surface area occupied by plaque was measured at 6 weeks in *Col8^{+/+};ApoE^{-/-}* (n = 14) and *Col8^{-/-};ApoE^{-/-}* (n = 13) mice or at 12 weeks in *Col8^{+/+};ApoE^{-/-}* (n = 11) and *Col8^{-/-};ApoE^{-/-}* (n = 16) mice. Black bars represent values from *Col8^{+/+};ApoE^{-/-}* mice, and hatched bars represent values from *Col8^{-/-};ApoE^{-/-}* mice. Values are given as means ± SEM. Scale bars: 100 μm .

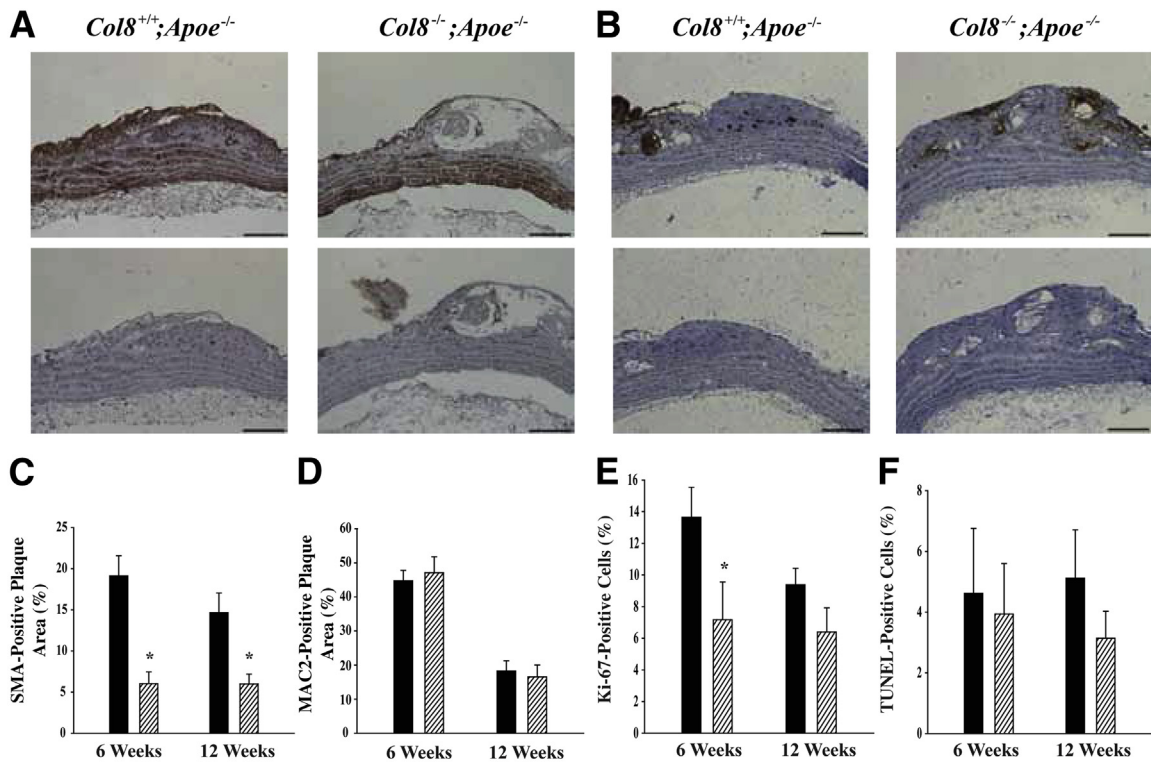


Figure 4 SMC accumulation and proliferation are reduced in *Col8^{-/-};ApoE^{-/-}* mice. Representative longitudinal sections of the lesser curvature of the aortic arch after 12 weeks of an atherogenic diet and stained with antibody against α -smooth muscle actin (A) or antibody against Mac-2 to label macrophages (B), along with their respective negative controls. C: Percentage of plaque area stained positive for SMA at 6 weeks in *Col8^{+/+};ApoE^{-/-}* ($n = 11$) and *Col8^{-/-};ApoE^{-/-}* ($n = 10$) mice or at 12 weeks in *Col8^{+/+};ApoE^{-/-}* ($n = 9$) and *Col8^{-/-};ApoE^{-/-}* ($n = 8$) mice. * $P \leq 0.05$ comparing genotypes at the same time point. D: Percentage of plaque area stained positive for Mac-2 at 6 weeks in *Col8^{+/+};ApoE^{-/-}* ($n = 13$) and *Col8^{-/-};ApoE^{-/-}* ($n = 13$) mice or at 12 weeks in *Col8^{+/+};ApoE^{-/-}* ($n = 7$) and *Col8^{-/-};ApoE^{-/-}* ($n = 8$) mice. E: Percentage of proliferating cells at 6 weeks in *Col8^{+/+};ApoE^{-/-}* ($n = 8$) and *Col8^{-/-};ApoE^{-/-}* ($n = 11$) mice or at 12 weeks in *Col8^{+/+};ApoE^{-/-}* ($n = 13$) and *Col8^{-/-};ApoE^{-/-}* ($n = 7$) mice. * $P \leq 0.05$ comparing genotypes at the same time point. F: Percentage of apoptotic cells at 6 weeks in *Col8^{+/+};ApoE^{-/-}* ($n = 7$) and *Col8^{-/-};ApoE^{-/-}* ($n = 12$) mice or at 12 weeks in *Col8^{+/+};ApoE^{-/-}* ($n = 9$) and *Col8^{-/-};ApoE^{-/-}* ($n = 8$) mice. Black bars represent values from *Col8^{+/+};ApoE^{-/-}* mice, and hatched bars represent values from *Col8^{-/-};ApoE^{-/-}* mice. Values are given as means \pm SEM. Scale bars: 100 μ m.

media and those migrating into the neointima; however, those studies did not resolve the functional importance of this expression.^{3,4} We show herein that after femoral injury in the absence of type VIII collagen, SMC apoptosis was increased, whereas migration to the intima was decreased, resulting in a reduction in cell number and decreased vessel wall thickening, as compared with the response in *Col8^{+/+}* mice. Because medial SMC proliferation was increased in *Col8^{-/-}* mice, decreased cell number could not be explained by reduced proliferation of this cell population. Rather, our data suggest that type VIII collagen contributes to vessel thickening by protecting SMCs from apoptosis and stimulating their migration. The femoral arteries of *Col8^{+/+}* mice underwent substantial outward remodeling, as evidenced by expansion of vessel diameter. However, femoral arteries from *Col8^{-/-}* mice did not substantially increase in vessel diameter after injury, thus exhibiting less potential for outward remodeling.

Expression of type VIII collagen has previously been noted in plaques from *ApoE^{-/-}* mice.⁵ We report here for the first time that ApoE regulates type VIII collagen expression. In humans, progression of atherosclerosis is accompanied by a decrease in plasma HDL concentration, the primary carrier

of ApoE. Herein we show that loss of ApoE results in up-regulation of type VIII collagen expression in the vessel wall. This is mediated by a direct effect on SMCs because treatment of cultured cells with ApoE or HDL suppressed mRNA expression for type VIII collagen. Early work revealed that ApoE can protect against atherosclerosis independent of cholesterol transport,²⁵ and subsequent cell culture studies have identified cholesterol-independent effects of ApoE (reviewed in Hui and Basford¹⁷). However, few of these studies have documented protection *in vivo*. The mechanisms by which ApoE regulates type VIII collagen expression are not known; however, one possibility is through modulation of cyclooxygenase-2 and prostacyclin.^{18,26} Another important atherogenic lipoprotein also regulates type VIII collagen expression; Cherepanova et al¹² showed that oxidized LDL but not native LDL stimulates type VIII collagen synthesis by SMCs *in vitro*. Considered together, these studies identify type VIII collagen as a target for two of the most potent atherogenic risk factors. It is noteworthy that the extracellular matrix provides a depot for accumulation of lipoproteins in atheromas, and these lipoproteins can in turn exert feedback regulation of matrix

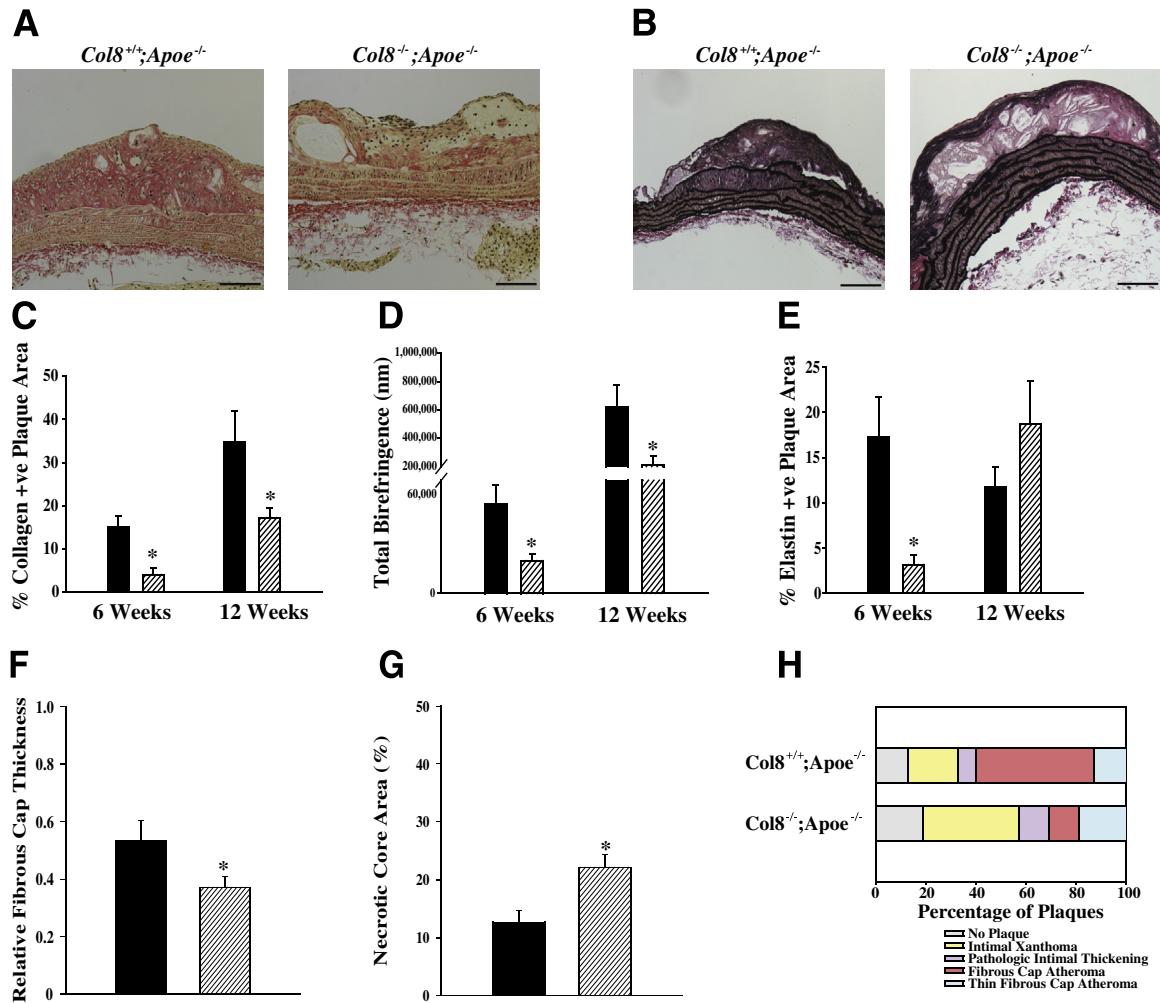


Figure 5 Matrix accumulation and fibrous cap thickness are decreased, and plaque necrotic core size is increased in plaques from *Col8^{-/-};ApoE^{-/-}* mice. Representative longitudinal sections of plaques from the lesser curvature of the aortic arch after 12 weeks of an atherogenic diet and stained with PSR to label collagen (A) or Verhoeff–van Gieson to label elastin (B). C: Percentage of plaque area stained positive with PSR at 6 weeks in *Col8^{+/+};ApoE^{-/-}* ($n = 12$) and *Col8^{-/-};ApoE^{-/-}* ($n = 13$) mice or at 12 weeks in *Col8^{+/+};ApoE^{-/-}* ($n = 9$) and *Col8^{-/-};ApoE^{-/-}* ($n = 8$) mice. D: Fibrillar collagen content, measured as birefringence via PolScope at 6 weeks in *Col8^{+/+};ApoE^{-/-}* ($n = 12$) and *Col8^{-/-};ApoE^{-/-}* ($n = 13$) mice or at 12 weeks in *Col8^{+/+};ApoE^{-/-}* ($n = 9$) and *Col8^{-/-};ApoE^{-/-}* ($n = 8$) mice. E: Percentage of elastin-positive plaque area at 6 weeks in *Col8^{+/+};ApoE^{-/-}* ($n = 7$) and *Col8^{-/-};ApoE^{-/-}* ($n = 15$) mice or at 12 weeks in *Col8^{+/+};ApoE^{-/-}* ($n = 8$) and *Col8^{-/-};ApoE^{-/-}* ($n = 7$) mice. F: Relative fibrous cap thickness in *Col8^{+/+};ApoE^{-/-}* ($n = 11$) and *Col8^{-/-};ApoE^{-/-}* ($n = 8$) mice at 12 weeks. G: Percentage of plaque occupied by necrotic core in *Col8^{+/+};ApoE^{-/-}* ($n = 12$) and *Col8^{-/-};ApoE^{-/-}* ($n = 10$) mice at 12 weeks. Black bars represent values from *Col8^{+/+};ApoE^{-/-}* mice, and hatched bars represent values from *Col8^{-/-};ApoE^{-/-}* mice. Values are given as means \pm SEM. C–G: $*P \leq 0.05$ comparing genotypes at the same time point. H: Classification of lesions found at 12 weeks in *Col8^{+/+};ApoE^{-/-}* ($n = 15$) and *Col8^{-/-};ApoE^{-/-}* ($n = 16$) mice. Scale bars: 100 μ m.

production. Lipoproteins can also influence matrix assembly; for example, LDL loading in SMCs interferes with the machinery for fibronectin and collagen fibril assembly, which may compromise plaque stability.²⁷

Deletion of type VIII collagen in *ApoE^{-/-}* mice led to major changes in plaque architecture including decreases in SMC and type I collagen accumulation in the fibrous cap and pronounced thinning of the cap. Moreover, because knockout of type VIII collagen did not reduce macrophage accumulation, the plaques were rich in macrophages, giving rise to large accumulations of foam cells, which expanded the necrotic core. These changes in plaque structure occurred in the absence of substantial differences in plaque size and total

plaque burden, which suggests that accumulation of foam cells and lipids compensated for the loss of SMCs and collagen, resulting in similar plaque size but increased vulnerability. In humans, atherosclerotic plaques that are susceptible to rupture are characterized by thin fibrous caps and large lipid-rich necrotic cores, with abundant macrophages.²⁸ Our data suggest that type VIII collagen promotes growth of a strong protective fibrous cap and, therefore, may have an important role in plaque stabilization during atherosclerosis. We have not assessed plaque rupture in these mice, but this is an important direction for future research.

A common feature after type VIII collagen deletion in both the wire injury and *ApoE^{-/-}* atherosclerosis models

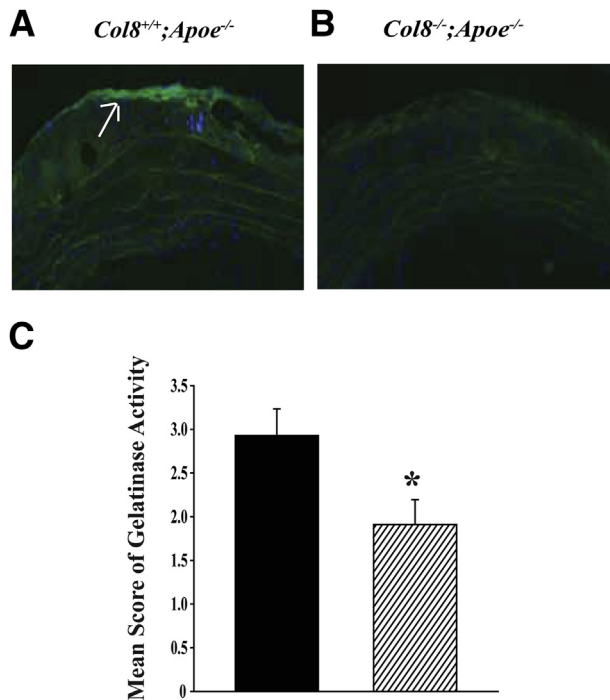


Figure 6 Plaque *in situ* gelatinase activity is decreased in $Col8^{-/-};ApoE^{-/-}$ mice. Representative longitudinal sections of plaques in the aortic arch from $Col8^{+/+};ApoE^{-/-}$ mice (A) or $Col8^{-/-};ApoE^{-/-}$ mice (B) after 12 weeks of an atherogenic diet. Bright green fluorescence represents the area of gelatinase activity (arrow in A). C: Average ranked score of gelatinase activity in the plaques. Black bars represent values from $Col8^{+/+};ApoE^{-/-}$ mice ($n = 6$), and hatched bars represent values from $Col8^{-/-};ApoE^{-/-}$ mice ($n = 8$). * $P \leq 0.05$ comparing genotypes.

was decreased SMC accumulation in the intimal layer. However, the mechanisms by which this occurred differed between the two models: there was decreased SMC proliferation in the atherosclerosis model and increased SMC proliferation but also increased apoptosis in the wire injury model. Inasmuch as lesion development progresses over a much longer time in atherosclerosis compared with wire injury, we cannot rule out the possibility that we have missed differences between genotypes by sampling at only two defined time points. However, there are other plausible explanations for the differences in the effects of type VIII collagen deletion on cell proliferation in the two models. First, the increased proliferation of medial SMCs in $Col8^{-/-}$ mice in the wire injury model could be an attempt to compensate for the cell loss due to the high rate of apoptosis. This model causes severe injury to cells in the media via the physical force exerted in stretching the vessel with the wire, and previous studies have reported concurrent increases in SMC proliferation and apoptosis after mechanical injury of arteries.^{29,30} Second, because there is little inflammation in the femoral artery injury model, type VIII collagen acts on SMCs alone and seems to inhibit SMC proliferation. In contrast, in the atherosclerotic model, type VIII collagen may stimulate plaque macrophages to express various cytokines and growth factors known to increase

SMC proliferation.¹¹ Thus, in the absence of type VIII collagen, there could be less cytokine production and less paracrine stimulation of SMC proliferation.

Regardless of differences in the mechanisms controlling proliferation, we propose that a similar mechanism underpins type VIII collagen-dependent SMC migration in both models. New type VIII collagen is deposited on top of type I collagen and/or other interstitial matrix, thus functioning as a provisional matrix enabling cell migration and stimulating matrix-degrading proteinases that facilitate movement. This is consistent with previous work *in vitro* from Pickering and colleagues, who demonstrated that both synthesis of new collagen and degradation of existing collagen were required for SMC migration.^{31,32} It is also consistent with our previous work that showed that type VIII collagen stimulated migration and MMP-2 activity in SMCs and that SMCs isolated from $Col8^{-/-}$ mice elaborated less MMP-2 activity than did those from $Col8^{+/+}$ mice.^{14,15} Other groups have identified a crucial role for MMP-2 in SMC migration during intimal thickening and atherosclerotic plaque development.^{33–35} In the present study, we have shown that there is decreased proteolytic activity in plaques from $Col8^{-/-};ApoE^{-/-}$ mice. Thus, we propose that the thin fibrous caps in $Col8^{-/-};ApoE^{-/-}$ mice are due, at least in part, to impaired MMP-2-dependent SMC migration into the plaque, with a consequent reduction in fibrillar collagen deposition to strengthen the cap. Accordingly, in the $Col8^{-/-};ApoE^{-/-}$ plaques, there was decreased fibrillar collagen birefringence and decreased immunostaining for the fibrillar type I collagen. Type VIII collagen has been localized to the fibrous cap in $ApoE^{-/-}$ mice⁵; however, because it is a nonfibrillar collagen, the decrease in fibrillar collagen observed in the caps of $Col8^{-/-};ApoE^{-/-}$ mice cannot be attributed to lack of type VIII collagen. However, type VIII collagen is known to associate with other collagens, elastin microfibrillar proteins, and proteoglycans,^{36–38} therefore is possible that it facilitates the assembly of other matrix components in the cap.

Previous studies have identified type VIII collagen production by macrophages *in vitro*, and *in situ* hybridization for type VIII collagen mRNA was co-localized with macrophages in atherosclerotic plaques in humans.⁷ However, our data do not support a role for type VIII collagen influencing plaque macrophage accumulation in the $ApoE^{-/-}$ mouse model. It is possible that type VIII collagen produced by macrophages exerts paracrine effects, attracting SMCs to the lesion or stimulating proliferation. It is also possible that type VIII collagen has other functions related to inflammation in atherosclerosis; however, little is known about this at present.

In conclusion, compared with $Col8^{+/+}$ mice, $Col8^{-/-}$ mice exhibit decreased vessel wall thickening and reduced outward vessel remodeling after femoral arterial injury. Deficiency of type VIII collagen in $ApoE^{-/-}$ mice results in impaired SMC proliferation and migration into the plaque and ultimately in development of atherosclerotic plaques with thin or absent fibrous caps. Thus, we have identified an

important mediator of fibrous cap thickening. Furthermore, we have identified an important role for ApoE in suppressing type VIII collagen expression in normal vessels. Together, our studies demonstrate an important role for type VIII collagen in mediating SMC infiltration into the intima *in vivo* after arterial injury or disease. However, there are distinct implications of these findings; for example, although inhibition of type VIII collagen may be desirable to limit expansion of SMC-rich lesions in transplant arteriopathy, this strategy cannot be applied to treatment of primary atherosclerosis, in which care should be taken to preserve type VIII collagen and the stability of the fibrous cap.

Acknowledgments

We thank Dr. Bjorn Olsen for providing mice, Hangjun Zhang for measurement of mean arterial pressure and heart rate, and Drs. Michael C. Phillips and Sissel Lund-Katz for providing lipoprotein.

Supplemental Data

Supplemental material for this article can be found at <http://dx.doi.org/10.1016/j.ajpath.2013.02.011>.

References

- Adiguzel E, Ahmad PJ, Franco C, Bendeck MP: Collagens in the progression and complications of atherosclerosis. *Vasc Med* 2009, 14: 73–89
- Bendeck MP, Regenass S, Tom WD, Giachelli CM, Schwartz SM, Hart C, Reidy MA: Differential expression of alpha 1 type VIII collagen in injured platelet-derived growth factor-BB-stimulated rat carotid arteries. *Circ Res* 1996, 79:524–531
- Sibinga NE, Foster LC, Hsieh CM, Perrella MA, Lee WS, Endege WO, Sage EH, Lee ME, Haber E: Collagen VIII is expressed by vascular smooth muscle cells in response to vascular injury. *Circ Res* 1997, 80:532–541
- Sinha S, KIELTY CM, Heagerty AM, Canfield AE, Shuttleworth CA: Upregulation of collagen VIII following porcine coronary artery angioplasty is related to smooth muscle cell migration not angiogenesis. *Int J Exp Pathol* 2001, 82:295–302
- Yasuda O, Zhang SH, Miyamoto Y, Maeda N: Differential expression of the alpha1 type VIII collagen gene by smooth muscle cells from atherosclerotic plaques of apolipoprotein-E-deficient mice. *J Vasc Res* 2000, 37:158–169
- Plenz G, Dorszewski A, Breithardt G, Robenek H: Expression of type VIII collagen after cholesterol diet and injury in the rabbit model of atherosclerosis. *Arterioscler Thromb Vasc Biol* 1999, 19:1201–1209
- Weitkamp B, Cullen P, Plenz G, Robenek H, Rauterberg J: Human macrophages synthesize type VIII collagen *in vitro* and in the atherosclerotic plaque. *FASEB J* 1999, 13:1445–1457
- MacBeath JR, KIELTY CM, Shuttleworth CA: Type VIII collagen is a product of vascular smooth-muscle cells in development and disease. *Biochem J* 1996, 319(Pt 3):993–998
- Plenz G, Dorszewski A, Völker W, Ko YS, Severs NJ, Breithardt G, Robenek H: Cholesterol-induced changes of type VIII collagen expression and distribution in carotid arteries of rabbit. *Arterioscler Thromb Vasc Biol* 1999, 19:2395–2404
- Qiu H, Depre C, Ghosh K, Resuello RG, Natividad FF, Rossi F, Peppas A, Shen YT, Vatner DE, Vatner SF: Mechanism of gender-specific differences in aortic stiffness with aging in nonhuman primates. *Circulation* 2007, 116:669–676
- Plenz G, Deng MC, Robenek H, Völker W: Vascular collagens: spotlight on the role of type VIII collagen in atherogenesis. *Atherosclerosis* 2003, 166:1–11
- Cherepanova OA, Pidkivka NA, Sarmiento OF, Yoshida T, Gan Q, Adiguzel E, Bendeck MP, Berliner J, Leitinger N, Owens GK: Oxidized phospholipids induce type VIII collagen expression and vascular smooth muscle cell migration. *Circ Res* 2009, 104:609–618
- Garvey SM, Sinden DS, Schoppee Bortz PD, Wamhoff BR: Cyclosporine up-regulates Krüppel-like factor-4 (KLF4) in vascular smooth muscle cells and drives phenotypic modulation *in vivo*. *J Pharmacol Exp Ther* 2010, 333:34–42
- Hou G, Mulholland D, Gronska MA, Bendeck MP: Type VIII collagen stimulates smooth muscle cell migration and matrix metalloproteinase synthesis after arterial injury. *Am J Pathol* 2000, 156:467–476
- Adiguzel E, Hou G, Mulholland D, Hopfer U, Fukai N, Olsen BR, Bendeck MP: Migration and growth are attenuated in vascular smooth muscle cells with type VIII collagen-null alleles. *Arterioscler Thromb Vasc Biol* 2006, 26:56–61
- Zhu Y, Bellosa S, Langer C, Bernini F, Pitas RE, Mahley RW, Assmann G, von Eckhardstein A: Low-dose expression of a human apolipoprotein E transgene in macrophages restores cholesterol efflux capacity of apolipoprotein E-deficient mouse plasma. *Proc Natl Acad Sci USA* 1998, 95:7585–7590
- Hui DY, Basford JE: Distinct signaling mechanisms for apoE inhibition of cell migration and proliferation. *Neurobiol Aging* 2005, 26:317–323
- Kothapalli D, Fuki I, Ali K, Stewart SA, Zhao L, Yahil R, Kwiatkowski D, Hawthorne EA, FitzGerald GA, Phillips MC, Lund-Katz S, Puré E, Rader DJ, Assoian RK: Antimitogenic effects of HDL and APOE mediated by Cox-2-dependent IP activation. *J Clin Invest* 2004, 113:609–618
- Hopfer U, Fukai N, Hopfer H, Wolf G, Joyce N, Li E, Olsen BR: Targeted disruption of Col8a1 and Col8a2 genes in mice leads to anterior segment abnormalities in the eye. *FASEB J* 2005, 19:1232–1244
- Sata M, Maejima Y, Adachi F, Fukino K, Saiura A, Sugiura S, Aoyagi T, Imai Y, Kurihara H, Kimura K, Omata M, Makuuchi M, Hirata Y, Nagai R: A mouse model of vascular injury that induces rapid onset of medial cell apoptosis followed by reproducible neointimal hyperplasia. *J Mol Cell Cardiol* 2000, 32:2097–2104
- Klein EA, Yung Y, Castagnino P, Kothapalli D, Assoian RK: Cell adhesion, cellular tension, and cell cycle control. *Methods Enzymol* 2007, 426:155–175
- Virmani R, Kolodgie FD, Burke AP, Farb A, Schwartz SM: Lessons from sudden coronary death: a comprehensive morphological classification scheme for atherosclerotic lesions. *Arterioscler Thromb Vasc Biol* 2000, 20:1262–1275
- Zhu B, Kuhel DG, Witte DP, Hui DY: Apolipoprotein E inhibits neointimal hyperplasia after arterial injury in mice. *Am J Pathol* 2000, 157:1839–1848
- Deguchi JO, Aikawa M, Tung CH, Aikawa E, Kim DE, Ntziachristos V, Weissleder R, Libby P: Inflammation in atherosclerosis: visualizing matrix metalloproteinase action in macrophages *in vivo*. *Circulation* 2006, 114:55–62
- Thorngate FE, Yancey PG, Kellner-Weibel G, Rudel LL, Rothblat GH, Williams DL: Testing the role of apoA-I, HDL, and cholesterol efflux in the atheroprotective action of low-level apoE expression. *J Lipid Res* 2003, 44:2331–2338
- Ali K, Lund-Katz S, Lawson J, Phillips MC, Rader DJ: Structure-function properties of the apoE-dependent COX-2 pathway in vascular smooth muscle cells. *Atherosclerosis* 2008, 196:201–209
- Frontini MJ, O'Neil C, Sawyez C, Chan BM, Huff MW, Pickering JG: Lipid incorporation inhibits Src-dependent assembly of fibronectin and type I collagen by vascular smooth muscle cells. *Circ Res* 2009, 104: 832–841

28. Libby P: The molecular mechanisms of the thrombotic complications of atherosclerosis. *J Intern Med* 2008, 263:517–527
29. Han DK, Haudenschild CC, Hong MK, Tinkle BT, Leon MB, Liao G: Evidence for apoptosis in human atherogenesis and in a rat vascular injury model. *Am J Pathol* 1995, 147:267–277
30. Bochaton-Piallat ML, Gabbiani F, Redard M, Desmoulière A, Gabbiani G: Apoptosis participates in cellularity regulation during rat aortic intimal thickening. *Am J Pathol* 1995, 146:1059–1064
31. Li S, Chow LH, Pickering JG: Cell surface-bound collagenase-1 and focal substrate degradation stimulate the rear release of motile vascular smooth muscle cells. *J Biol Chem* 2000, 275:35384–35392
32. Rocnik EF, Chan BM, Pickering JG: Evidence for a role of collagen synthesis in arterial smooth muscle cell migration. *J Clin Invest* 1998, 101:1889–1898
33. Johnson C, Galis ZS: Matrix metalloproteinase-2 and -9 differentially regulate smooth muscle cell migration and cell-mediated collagen organization. *Arterioscler Thromb Vasc Biol* 2004, 24:54–60
34. Kuzuya M, Kanda S, Sasaki T, Tamaya-Mori N, Cheng XW, Itoh T, Itohara S, Iguchi A: Deficiency of gelatinase a suppresses smooth muscle cell invasion and development of experimental intimal hyperplasia. *Circulation* 2003, 108:1375–1381
35. Kuzuya M, Nakamura K, Sasaki T, Cheng XW, Itohara S, Iguchi A: Effect of MMP-2 deficiency on atherosclerotic lesion formation in apoE-deficient mice. *Arterioscler Thromb Vasc Biol* 2006, 26:1120–1125
36. Iruela-Arispe ML, Chun LE, Sage EH: [Structure and biology of type VIII collagen], Japanese. *Trends Glycosci Glycotechnol* 1992, 4:188–199
37. Suttmuller M, Bruijn JA, de Heer E: Collagen types VIII and X, two non-fibrillar, short-chain collagens: structure homologies, functions and involvement in pathology. *Histol Histopathol* 1997, 12:557–566
38. Sawada H, Konomi H: The alpha 1 chain of type VIII collagen is associated with many but not all microfibrils of elastic fiber system. *Cell Struct Funct* 1991, 16:455–466